King Saud University

Arabian Journal of Chemistry

www.ksu.edu.sa
www.sciencedirect.com

ORIGINAL ARTICLE

Synthesis and characterization of FeTiO$_3$ ceramics

CrossMark

Anil B. Gambhire [a], Machhindra K. Lande [b,*], Sandip B. Rathod [b], Balasaheb R. Arbad [b], Kaluram N. Vidhate [b], Ramakrishna S. Gholap [c], Kashinath R. Patil [c]

[a] *Department of Chemistry, Shri Anand College of Science, Pathardi, Ahmednagar 414102, India*
[b] *Department of Chemistry, Dr. Babasaheb Ambedkar Marathwada University, Aurangabad 431004, Maharashtra, India*
[c] *Catalysis Division, National Chemical Laboratory, Pashan Road, Pune 411008, India*

Abstract   Nanocrystalline FeTiO$_3$ ceramics powders were prepared by the sol–gel process combined with a surfactant-assisted template method. The resulting powders were calcined at different temperatures ranging from 150 °C to 600 °C for 2 h in an air. The results revealed that a pure hexagonal phase of FeTiO$_3$ could be obtained at low temperature, 600 °C. The phase evolution of FeTiO$_3$ was investigated by X-ray diffraction patterns (XRD), Fourier-transform infrared spectroscopy (FT-IR), and X-ray photoelectron spectroscopy (XPS). Particle size and morphology was studied by transmission electron microscopy (TEM).

© 2011 Production and hosting by Elsevier B.V. on behalf of King Saud University. This is an open access article under the CC BY-NC-ND license (http://creativecommons.org/licenses/by-nc-nd/3.0/).

1. Introduction

Wide band gap semiconductors are of interest due to their potential applications in a large number of novel devices such as radiation immune solar cells, high temperature integrated circuits and high power electronic devices (Ginley and Butler, 1977; Zhou et al., 2002). FeTiO$_3$ is a wide band gap (2.54 eV) antiferromagnetic semiconductor material having potential applications in spintronics with a Curie temperature of 1000 K (Dai et al., 1999; Zhou et al., 2003; Fujii et al., 2004a,b). Motivated by these applications, numerous efforts have been made to control the size and shape of FeTiO$_3$ ceramics. The structure of FeTiO$_3$ (space group $R\bar{3}$) is similar to that of hematite (α-Fe$_2$O$_3$), where the two Fe^{3+} ions in hematite are replaced by Fe^{2+} and Ti^{4+} in ilmenite in ordered way along the c-axis. The present advancement in microelectronics and communication systems is gradually leading to the miniaturization of antiferromagnetic materials. The quality of ceramic semiconductor can be improved through smaller-sized components. In order to achieve high antiferromagnetic semiconducting property in a small volume, the particle size has to be reduced. Thus, the interest in high-quality FeTiO$_3$ nanopowders with narrow particle size distribution is continuously increasing.

* Corresponding author. Tel.: +91 0240 2403311; fax: +91 0240 2403335.
E-mail address: mkl_chem@ymail.com (M.K. Lande).
Peer review under responsibility of King Saud University.

Production and hosting by Elsevier

Recently, FeTiO$_3$ oxide powder prepared by co-precipitation of mixed metal oxalate is reported in the literature (Sharma et al., 2009). Similarly, other methods like citrate gel technique (Dhage et al., 2003; Dhage et al., 2004a,b; Gaikwad et al., 2004); liquid mix and H$_2$/H$_2$O reduction process (Tang and Hu, 2006); solid sate reaction (Naylor and Cook, 1946; Grant et al., 1972); using different chemical techniques at 400 °C are also reported in the literature (Mona et al., 2006). It has been observed that given crystallite size of the final product is larger (Sharma et al., 2009; Dhage et al., 2003; Dhage et al., 2004a,b; Gaikwad et al., 2004; Tang and Hu, 2006; Naylor and Cook, 1946; Grant et al., 1972; Mona et al., 2006); which will reduce the quality of ceramic semiconductor. The solid sate reaction method is generally based on mixing of fine powders and heating at very higher temperature leads to inhomogeneity. However, the sol–gel process is one of the most successful techniques for the synthesis of nanosize ceramic powders, producing a narrow particle size distribution and showing considerable advantages over the above reported methods. These advantages include excellent compositional control, homogeneity on the molecular level due to the mixing of liquid precursor, and lower crystallization temperature. In the earlier studies, FeTiO$_3$ were prepared by co-precipitation, citrate gel, liquid mix process, solid sate reaction and hydrothermal method with larger particle size in the range of 40–100 nm obtained below 400 °C (Mona et al., 2006), and 600 °C (Sharma et al., 2009; Dhage et al., 2003; Dhage et al., 2004a,b; Gaikwad et al., 2004; Tang and Hu, 2006; Naylor and Cook, 1946; Grant et al., 1972), might be due to improper crystallization of precursor. In the present investigation we have prepared FeTiO$_3$ ceramics using sol–gel method in combination with surfactant-assisted template so as to have nanoparticles of FeTiO$_3$ ceramics with desired dimensions at 600 °C. Surfactant-template method was widely used to synthesize nanoscale ceramic powders (Beck et al., 1992; Ying et al., 1999; Tanev et al., 1997). With the success of surfactant-templating synthesis of MCM-like material (Yin et al., 2007; Liu et al., 2007); it is believed that nanoparticles of FeTiO$_3$ ceramics could be possible to synthesize using similar surfactant synthetic strategy. We have used the cationic surfactant cetyltrimethylammonium bromide (CTAB) as a structure directing agent by mixing it in an alkoxide solution in order to modify the microstructure of the gels, which will certainly allow the formation of oxides with controlled particle size.

2. Experimental

Precursor solutions were prepared by the following method. An aqueous solution of 0.12 M Fe(NO$_3$)$_3$·9H$_2$O was prepared using ethanol. The exact molarity of the solution was determined from the chemical analysis of the nitrate solution using solochrome Black-T indicator and standard EDTA solution. Required amount (Fe/Ti = 1:1) of Ti(OC$_4$H$_9$)$_4$ was added to the Fe(NO$_3$)$_3$·9H$_2$O solution with constant stirring. The cationic surfactant CTAB (10% (20 ml) in ethanol) was dropped into the solution. Then nitric acid (0.1 M) was added drop wise into the mixed solution so as to obtain a pH of 1–2. Stirring for 20 min resulted in the formation of a sol with dark brown color. The sol was then heated slowly up to 70 °C and dried to produce a brown fluffy porous gel. The dried gels were calcined at different temperatures ranging from 150 to 600 °C for 2 h in an air.

The X-ray diffraction (XRD) patterns were recorded with a Bruker 8D advanced X-ray diffractometer using monochromatic Cu K$_\alpha$ radiation (40 kV and 30 mA). The Fourier-transform infrared spectroscopy (FT-IR) analysis was performed using a Shimadzu-8400 spectrometer. The microscopic nanostructures were observed using a transmission electron microscopy (TEM; FEI, Tecnai F30, HRTEM, FEG operated at 300 kV). The fine powders were dispersed in amyl acetate on a carbon-coated TEM copper grid. For the determination of lattice parameters and interplanar distance d, the samples were scanned in the 2θ range of 20–80° for the period of 5 s in the step scan mode. Silicon was used as an internal standard. Least-squares analysis was employed to determine the lattice parameters. X-ray photoelectron spectroscopy (XPS) was used to study the chemical composition of the sample. The monochromatic X-ray beams of Al K$_\alpha$ (hv = 1486.6 eV) and Mg K$_\alpha$ (hv = 1253.6 eV) radiations were used as the excitation source. A hemispherical sector analyzer and multi channel detectors were used to detect the ejected photoelectrons as a function of their kinetic energies. XPS spectra were recorded at pass energy of 50 eV, 5 mm slit width and a take-off angle of 55°. The spectrometer was calibrated by determining the binding energies values of Au 4f$_{7/4}$ (84.0 eV), Ag 3d$_{5/2}$ (368.4 eV) and Cu 2P$_{3/2}$ (932.6 eV) levels using spectrograde materials. The instrumental resolution under these conditions was 1.6 eV full-width at half-maximum (FWHM) for Au 4f$_{7/4}$ level. The Cls (285 eV) and Au 4f$_{7/4}$ (84.0 eV) were used as internal standards when-ever needed. Thermo gravimetric analysis (TG) and differential scanning calorimetric analysis (DSC) was carried out simultaneously in a static N$_2$ atmosphere, using a Netzsch STA 409 instrument.

3. Results and discussion

Fig. 1 shows the XRD patterns of the as-prepared gel and those calcined at 150, 300, 500 and 600 °C, respectively. It can be seen from the diffraction patterns that the starting powders were amorphous with no significant change in structure up to 300 °C was observed. After calcinations at 500 °C, it was observed that the crystallization of the dried gel begun at this temperature along with the formation of anatase phase at 2θ = 25.32°, 48.06°, 55.09° and 62.16° and a rutile phase at 2θ = 27.44°, 36.09°, 41.25° and 44.05°. Further, by increasing the calcinations temperature to 600 °C, the XRD pattern indicates the formation of pure FeTiO$_3$ with hexagonal crystal structure according to JCPDS; 75-1207. The calculated lattice parameters by least squares fit are a = 5.141 Å and c = 14.22 Å. The particle size calculated from Scherrer's formula ($t = K\lambda/B\cos\theta_B$), where t is the average size of the particles, K = 0.9, λ is the wavelength of X-ray radiation, B is the full width at half maximum of the diffracted peak and θ_B is the angle of diffraction. The average particle size of FeTiO$_3$ powder calcined at 600 °C was around 25 nm.

Fig. 2 shows a TEM image for the sample calcined at 600 °C. It can be observed that the particle morphology is nearly spherical and of uniform size with limited aggregation. It has narrow particle size distribution ranging between 23 and 25 nm. The results are consistent with the XRD data.

Fig. 3 shows the FT-IR spectra of the as-prepared gel and those calcined at 150, 300, 500 and 600 °C, respectively. For the as-prepared gel and calcined samples, the broad band at
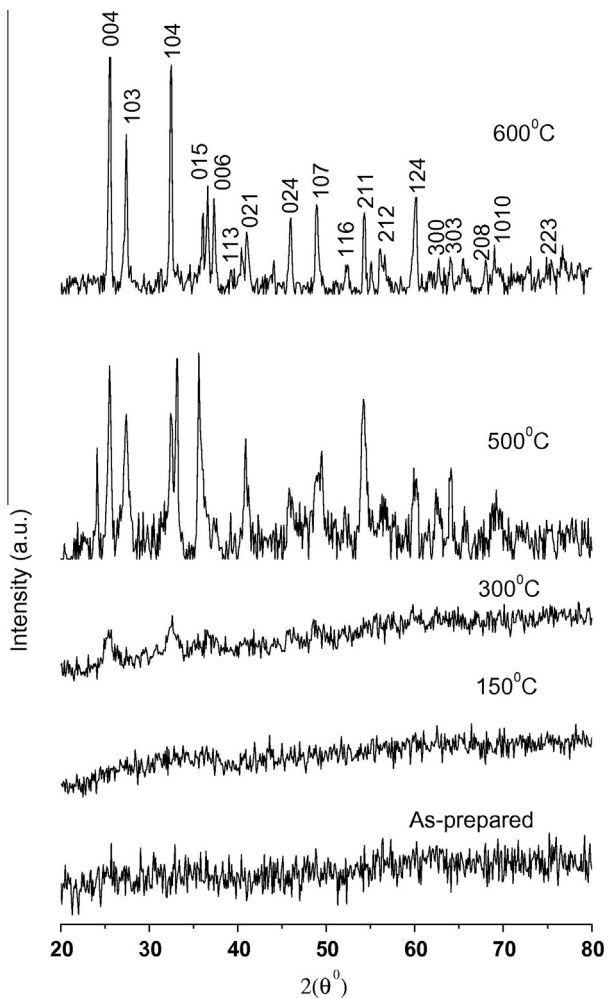
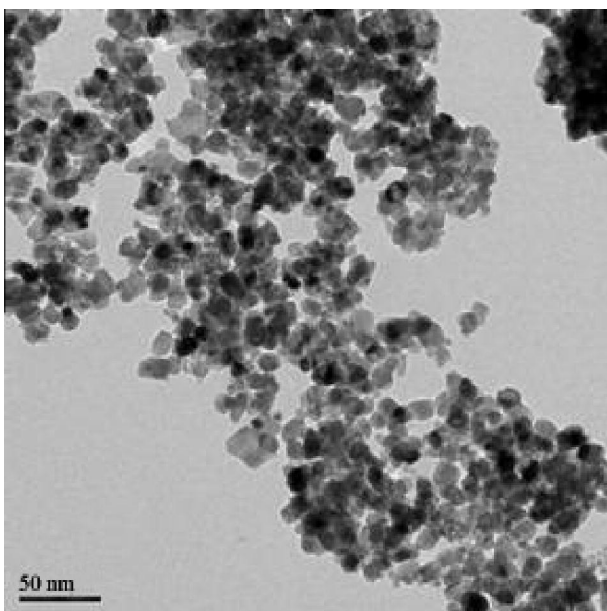**Figure 1** XRD patterns of powders calcined at different temperatures.

Figure 2 TEM of FeTiO₃ powder calcined at 600 °C.

$1627 \ cm^{-1}$ was attributed due to deformation mode of hydroxyl group from adsorbed water. Generally, the bands in the low-wave number region (400–650 cm^{-1}) can be assigned to Ti–O bond vibrations (Last, 1957). After calcinations at 600 °C, the absorption bands of Ti–O octahedral appeared at 680 and 500 cm^{-1}, corresponding to the formation of FeTiO₃.

Fig. 4 shows Fe 2p, Ti 2p and O 1s high-resolution XPS spectra of FeTiO₃ sample calcined at 600 °C for 2 h in an air. The Fe 2p and Ti 2p spectra shows peak positions at binding energies of 710.8 and 458.3 eV which correspond to elements in the oxidation states Fe^{3+} and Ti^{3+}, respectively.

The peak with an O 1s binding energy around 529.7 eV indicating that the oxygen atoms exist as O^{2-} species and that of at 531.8 eV indicating either adsorbed oxygen or hydroxyl species present on the surface of FeTiO₃.

Fig. 5 shows the thermal evolution of as prepared gels. Several components, such as physically adsorbed water and residual organic materials coming from the synthesis may be removed and assigned to different steps in the TG curve. Sharp weight losses are observed in two temperature ranges, the first between 50 and 250 °C and the second between 300 and 600 °C. The DSC curve displayed four corresponding valleys for as prepared gels. The first and second one appeared at
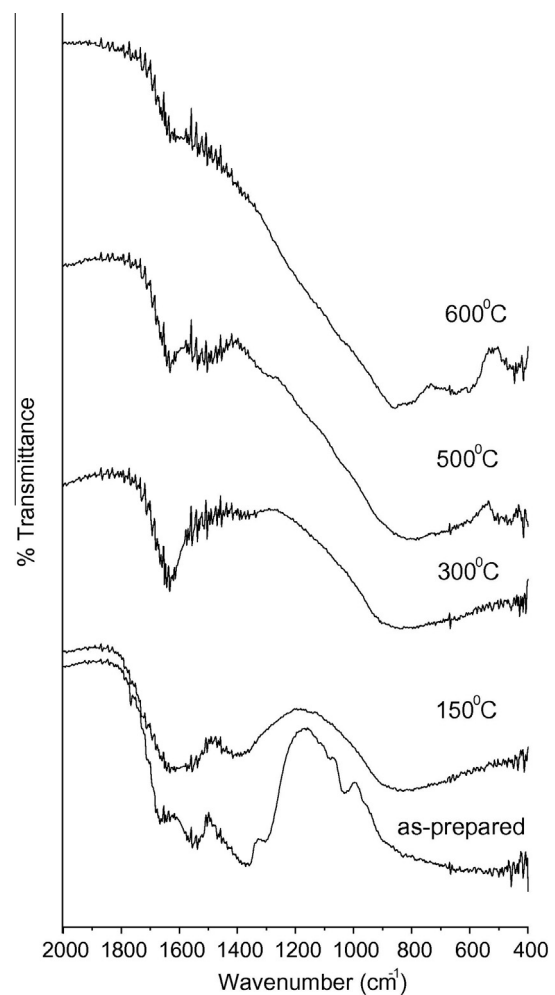

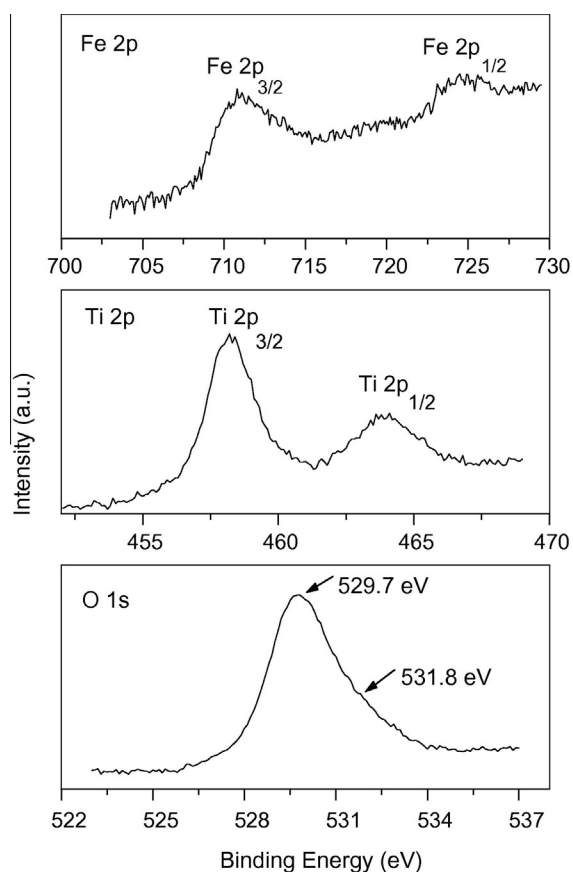**Figure 3** FT-IR spectra of FeTiO₃ powders calcined at different temperatures.

Figure 4 High resolution 2p and O 1s spectra of FeTiO$_3$ powder calcined at 600 °C.
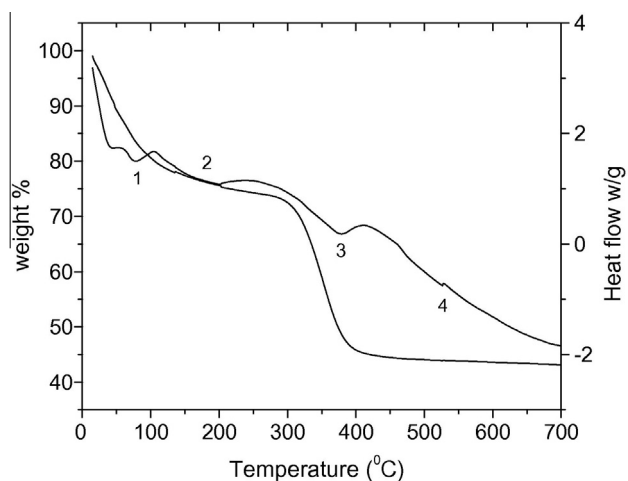

Figure 5 TG/DSC tracing of precursor gel.

about in the temperature region between 50 and 250 °C, which is ascribed to water desorption from the samples. The third one emerging at about 400 °C could be due to the dehydroxylation of Ti–OH into TiO^2 (Wang et al., 2001). The fourth one

emerging at about 540 °C, which indicates that the phase transformation of FeTiO$_3$ occurred as revealed by the XRD patterns.

Thus, it might be concluded that the FeTiO$_3$ formation was completed at 600 °C from the reaction between TiO$_2$ and Fe(NO$_3$)$_3$·9H$_2$O phases. These results are in good agreement with the XRD, FT-IR and TG-DSC data.

4. Conclusions

Nanosize FeTiO$_3$ ceramics have been successfully prepared by the sol–gel method combined with a surfactant-assisted template method. The formation of hexagonal phase of FeTiO$_3$ was detected by XRD, FT-IR and TG/DSC from the sample calcined at 600 °C. The FeTiO$_3$ particles were nearly spherical and uniform in size having a fairly narrow distribution in the range of 23–25 nm supported by both XRD and TEM.

References

Beck, J.S., Vartuli, J.C., Roth, W.J., Leonowicz, M.E., Kresge, C.T., Schmitt, K.D., 1992. J. Am. Chem. Soc. 114, 10834.
Dai, Z., Zhu, P., Yamamoto, S., Miyashita, A., Narum, K., Naramoto, H., 1999. Thin Solid Films 339, 114.
Dhage, S.R., Gaikwad, S.P., Muthukumar, P., Ravi, V., 2004a. Mater. Lett. 58, 2704.
Dhage, S.R., Khollam, Y., Dhesphande, S.B., Potdar, H.S., Ravi, V., 2004b. Mater. Res. Bull. 39, 1993.
Dhage, S.R., Pasricha, R., Ravi, R.V., 2003. Mater. Res. Bull. 38, 1623.
Fujii, T., Kayano, M., Takada, Y., Nakanishi, M., Takada, J., 2004a. Solid State Ion 172, 289.
Fujii, T., Kayano, M., Takada, Y., Nakanishi, M., Takada, J., 2004b. J. Magn. Magn. Mater. 272, 2010.
Gaikwad, S.P., Samuel, V., Pasricha, R., Ravi, V., 2004. Mater. Lett. 58, 3729.
Ginley, D.S., Butler, M.A., 1977. J. Appl. Phys. 48, 2019.
Grant, R.W., Hously, R.M., Geller, S., 1972. Phys. Rev. B 5, 1700.
Last, J.T., 1957. Phys. Rev. 105, 1740.
Liu, C., Yu, X., Yang, J., He, M., 2007. Mater. Lett. 61, 5261.
Mona, J., Kale, S.N., Gaikwad, A.B., Murugan, A.V., Ravi, V., 2006. Mater. Lett. 60, 1425.
Naylor, B.F., Cook, O.A., 1946. J. Am. Chem. Soc. 68, 1003.
Sharma, Y.K., Kharkwal, M., Uma, S., Nagarajan, R., 2009. Polyhedron 28, 579.
Tanev, P.T., Liang, Y., Pinnavaia, T.J., 1997. J. Am. Chem. Soc. 119, 8616.
Tang, X., Hu, K., 2006. J. Mater. Sci. 41, 8025.
Yin, L., Wang, F., Fu, J., 2007. Mater. Lett. 61, 3119.
Ying, J.Y., Mehnert, C.P., Wong, M.S., 1999. Angew. Chem. Int. Ed. 38, 56.
Zhou, F., Kotru, S., Pandey, R.K., 2002. Thin Solid Films 408, 33.
Zhou, F., Kotru, S., Pandey, R.K., 2003. Mater. Lett. 57, 2104.
Wang, X.W., Zhang, Z.Y., Zhou, S.X., 2001. Mater. Sci. Eng. 29, 33.